Adaptive Robotic Gait Control using Coupled Artificial Signalling Networks, Hopf Oscillators and Inverse Kinematics

Luis A. Fuente* †, Michael A. Lones* †, Alexander P. Turner* †,
Leo S. Caves* ‡, Susan Stepney* §, and Andy M. Tyrrell* †
†Department of Electronics, University of York, Heslington, York,YO10 5DD, UK
‡Department of Computer Science, University of York, Heslington, York, YO10 5DD, UK
§Department of Biology, University of York, Heslington, York, YO10 5DD, UK
*York Centre for Complex Systems Analysis (YCCSA)

***Abstract*—A novel bio-inspired architecture comprising three layers is introduced for a six-legged robot in order to generate adaptive rhythmic locomotion patterns using environmental information. Taking inspiration from the intracellular signalling processes that decode environmental information, and considering the emergent behaviours that arise from the interaction of multiple signalling pathways, we develop a decentralised robot controller composed of a collection of artificial signalling networks. Crosstalk, a biological signalling mechanism, is used to couple such networks favouring their interaction. We also apply nonlinear oscillators to model gait generators, which induce symmetric and rhythmical locomotion movements. The trajectories are modulated by a coupled artificial signalling network, which yields adaptive and stable robotic locomotive patterns. Gait trajectories are converted into joint angles by means of inverse kinematics. The architecture is implemented in a simulated version of the real robot T-Hex. Our results demonstrate the ability of the architecture to generate adaptive and periodic gaits.**

***Index Terms*—Evolution, Locomotion, Crosstalk, Oscillator, Coupling, Adaptation.**

I. Introduction

The necessity to survive causes living organisms to develop distinct abilities to interactively adapt to their surrounding environment. The capacity to orchestrate mechanisms to sense and respond to the environment is intrinsically difficult. In this respect, the role of cellular signalling in multicellular organisms is especially significant, since it underlies the coordination of complex multicellular interactions and the production of collective and adaptive responses. Cellular signalling is a sequence of biochemical reactions that are triggered by a chemical signal and lead to an adaptive cellular response. Signalling pathways are the fundamental structures connecting the environment to the genes they regulate, in turn producing a change in genes expression that brings about change in cellular activity. Crosstalk leads to interactions between signalling pathways, promoting the formation of larger biochemical networks which induce coordinated cellular responses with high robustness and sensitivity to environmental perturbations [1].

Locomotion is an example of a widespread adaptive response to environmental stimuli, permitting actions such us chasing prey, evading predators or exploring the environment. Locomotion is also important in robotics. Central Pattern Generators (CPGs) [2] are a common way of modelling, and in turn generating, locomotive gaits. Whilst they are often implemented using biologically-motivated models, such as feedforward neural networks [3] and artificial homeostatic systems [4], they can also be considered as systems of non-linear oscillators. Examples of this approach include [5], where coupled Van Der Pol (VDP) oscillators were used to dynamically modulate gaits in a quadruped robot; [6], which used a network of spring-like oscillators to model a crawling baby; and [7], where a non-linear oscillator-based CPG was used to achieve stability in bipedal walking robots. Other approaches include Rayleigh [8], Matsuoka [9] and Kuramoto [10] oscillators. The majority of these oscillators display a limit cycle, which offers resistance to small perturbations and generates smooth and periodic solutions.

Although consideration of environmental information is not essential in the generation of synchronised and rhythmic locomotion patterns, it increases the adaptability of control systems in real environments [2]. However, integrating environmental information is a hard task, particularly when these environmental signals come from multiple, diverse, and potentially noisy sources, such as the sensors mounted on robots. Nevertheless, it is a task that cellular signalling networks are evidently good at solving within a biological context. In this paper, we explore whether computational analogues of cellular signalling networks, which we refer to as artificial signalling networks (ASNs), can be used to solve an analogous task within a robotic system. In particular, we use an evolutionary algorithm to discover ASNs that, when stimulated with environmental information, modulate the parameters of a lower-level system of coupled oscillators, producing locomotive gaits which are then used to drive the inverse kinematics of a legged robot. In effect, this three-layered architecture uses sensory information to generate reactive behaviours that adaptively switch between the stance and swing phases in stepping

movements during locomotion. We applied this approach to the control of a simulated model of a commercial hexapod robot called the T-Hex [11]. In particular, coordinated control of the robot's six legs is handled using a collection of ASNs which are partially coupled together by crosstalk, a decentralised architecture inspired by the interactions amongst signalling pathways inside biological cells.

The paper is structured as follows: Section II presents the hierarchical architecture, describing each of its layers, Section III describes how the proposed bio-inspired controller is evolved, Section IV introduces the robotic locomotion task on which the robot is evaluated, Section V highlights the results and analysis and Section VI presents conclusions and discuses about future work.

II. System Overview

We introduce a hierarchical three-layer topology (see Fig. 1) in which a decentralised controller generates adaptive gait trajectories, which lead to rhythmical locomotion of a multi-legged robot.

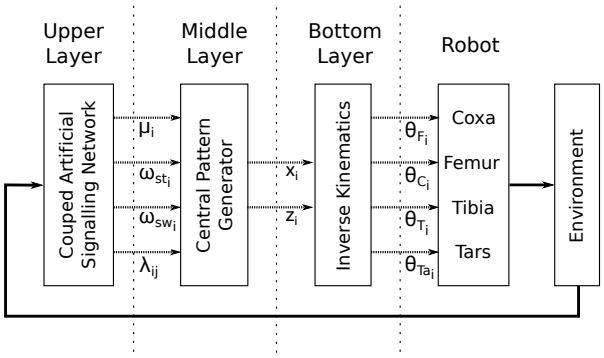

Fig. 1: Overview of the system topology. The network of CASNs modulates the parameters of the CPG's network. This generates gait trajectories, which are translated into robotic motion using inverse kinematics.

The upper layer comprises a coupled artificial signalling network (CASN). It receives environmental information from the robot's sensors and modulates the rhythmic parameters required for robot motion. Gait trajectories are generated in the middle layer. A network of CPG units, whose connectivity mirrors the CASN, receives parameters from the CASN and produces adaptive gait trajectories, one per leg. Finally, the bottom layer is fed with periodically sampled points of the trajectories, which an inverse kinematic model translates to the joint angles which drive the robot's locomotion.

A. Artificial Signalling Networks (ASN)

From a computational perspective, signalling networks have a number of interesting properties [12]. From the perspective of robotic locomotion, of particular significance is their ability to trigger robust, efficient and specific responses to environmental perturbations. A number of researchers have previously looked at how computational models of signalling networks might be applied to computational tasks [13], [14]. This includes a number of approaches which have used evolutionary algorithms to design the topology of the networks [13], [15].

In our previous work, we looked at the properties of a particular computational representation of signalling networks, and showed how this *artificial signalling network* could be used to solve chaos control tasks within numerical dynamical systems [16], [17]. This ASN is an abstraction of the patterns of interaction occurring between the molecules that constitute cellular signalling pathways. In addition to this, there is a focus on computational efficiency—most notably through the use of discrete time dynamics—and on computational expressiveness, notably through the use of continuous-valued functions and state variables.

Formally, an ASN consists of an indexed set of enzyme-analogous nodes, E, and a set of directed connections representing inhibitory and excitatory biochemical reactions, $\pm R$. Each $e_i \in E$ has a set of substrates S_i, a set of products P_i and a substrate-product mapping function, m_i. We used the *Michaelis-Menten* equation to regulate the kinematic reactions between enzymes, $m(c_i) = vc_i(k - c_i)$. It is an hyperbolic function where $v \in [0, 1]$ is its asymptotic threshold, $k \in [0, 1]$ its gradient and $c_i \in P_i$. Each reaction calculates its product concentration based on the substrate concentration of a set of enzymes. This approach extends the artificial metabolic network model described in [18]. The execution of an ASN starts with the random initialisation of its enzyme concentrations (S_i and P_i). External inputs are delivered to the network by setting the substrate concentrations of nominated enzymes. At each time step, each enzyme e_i applies its mapping function m_i to the current concentration of its substrate S_i to determine the current concentration of its product P_i. This new concentration is the mean output of all different contributing enzymes. For multiple inputs, $c_i = \sum_{e_j \in E_{c_i}} c_i^{e_j} / |E_{c_i}|$, where E_{c_i} is the set of enzymes for which $c_i^{e_j}$ is the output value of $e_j \in E$. Negative c_i values indicates inhibition, modelled as $c_i^- = 1 - c_i$. After iterating the network a specified number of times t_S, the outputs are extracted from the final product concentrations of nominated enzymes. For more detail, see [17].

B. Coupled Artificial Signalling Networks (CASN)

Biological responses are commonly the result of dynamical interactions amongst pathways, rather than the isolated action of an individual pathway. Motivated by this observation, a number of authors (including ourselves) have investigated the use of computational architectures based on models of interacting biochemical pathways [19]–[21]. Interactions can occur both between pathways of the same kind, and between pathways of different kinds. An example of the latter, which we explored in [19] in the context of robotic control, is the interaction between a metabolic pathway and a genetic pathway. However, in this work, we focus on interactions of signalling pathways with other signalling pathways, since this is the principal route through which biological organisms handle environmental interactions.

Crosstalk is an important mechanism underlying the joint response of signalling pathways. In the biological community, there has been a growing interest in crosstalk, stemming from the view that it acts as the glue in the development of complex interactive networks [22]. In [17], we considered a coupled ASN, in which nodes of different ASNs are connected through crosstalk. Formally, this CASN consists of an indexed set of ASNs and a set of crosstalk probabilities, C_p, each of which indicates the probability of exchanging information between neighbouring ASNs. Crosstalk connections can be either excitatory or inhibitory, and enzymes involved in crosstalk have their product concentration asymptotically reduced to half of their maximum value, mimicking the low reaction rates in crosstalk reactions within cells. The first time the CASN is executed, its chemical concentrations are randomly initialised and the crosstalk rates also randomly established, remaining constant during network execution. External inputs are delivered to designated ASN_i by setting the substrate concentrations of nominated enzymes. After a given period of time t_{S_i}, outputs are captured from the final product concentrations of nominated enzymes in each network.

In [17], this model was applied to a difficult control task. A key observation was that different inputs, although co-dependent, could be processed by different networks, with crosstalk interactions then enabling a joint response. This is a pattern of behaviour that seems particularly appropriate for robotic control, in which there are often many, potentially dependent, inputs. Figure 2 shows an example of an evolved CASN used in the upper layer of our three-layered architecture, showing how different groups of inputs are delivered to different ASNs and also the pattern of connections between ASNs which underlies their joint response.

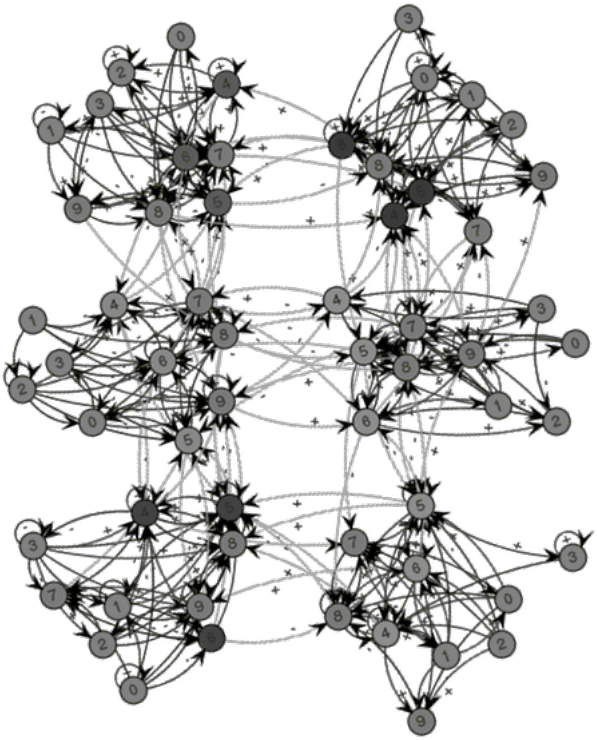

Fig. 2: Representation of a Coupled-Artificial Signalling Network. The network is composed of six independent ASNs, one per robot limb. Each network contains four inputs (low-numbered nodes) and three outputs (high-numbered nodes). Crosstalk is illustrated by the arcs connecting two neighboring ASNs.

C. Central Pattern Generator

The middle layer of the proposed topology models a CPG network that generates the rhythmic motion patterns needed for locomotion. The network is randomly initialized, and its parameters are modulated by the outputs of the CASN.

The movement of each limb is independently controlled by the x and z variables of the single nonlinear Hopf oscillator [23] as follows:

$$\begin{aligned} \dot{x_i} &= \alpha(\mu - r_i^2)x_i - \omega_i z_i \\ \dot{z_i} &= \beta(\mu - r_i^2)z_i + \omega_i x_i \end{aligned} \tag{1}$$

where x_i and z_i are state variables, $r_i = \sqrt{x_i^2 + z_i^2}$, the amplitude of the oscillator is given by $A = \sqrt{\mu}$ and the frequency of the oscillator (in $rad \cdot s^{-1}$) is governed by ω_i. α and β are positive constants that determine the velocity of convergence to the limited cycle. Figure 3 gives an example of a trajectory generated by a Hopf oscillator.

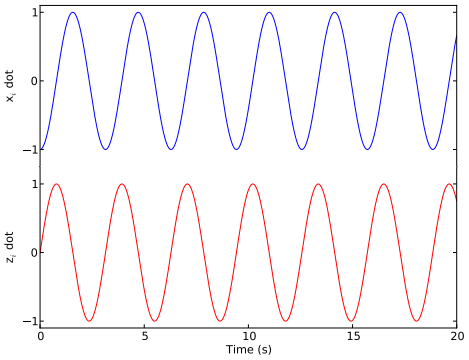

Fig. 3: Generated $\dot{x_i}$ (upper graph) and $\dot{z_i}$ (bottom graph) outputs of a Hopf oscillator, where $\omega = 4\,\text{rad} \cdot \text{s}^{-1}$, $\mu = 1$, $\alpha = 5$ and $\beta = 50$. The ascending and descending phases have the same frequency.

From our perspective, this oscillator has two prominent benefits. First, it is able to generate smooth, stable and cyclic trajectories in the presence of small perturbations to its parameters [24]. Secondly, the generated trajectory can be exclusively modulated by changing its amplitude, μ, and frequency, ω, whilst preserving the other parameters. This parameter separation eases their optimisation by evolutionary algorithms [25]. For example, in [26] the authors used an EA to optimise the gait parameters of a quadrupedal robot based on the robot's on-board sensors.

Compared to the work of [27], where the trajectory of a 3-

DOF limb is uniquely controlled by applying the $\dot{x}_i$ solution in the i-th coxa joint, we consider both solutions of the nonlinear oscillator, $\dot{x}_i$ and $\dot{z}_i$, to control the x- and z- coordinates respectively of the tip of each 4-DOF limb. This means that the tip of each limb mimics the generated trajectory of the ith oscillator.

The oscillator described in Eq. 1 produces an oscillatory trajectory where the ascending (swing) phase and the descending (stance) phase (see Fig. 3) have equal frequencies. In order to independently modulate the frequency of these parts, we utilise the following expression [6]:

$$\omega = \frac{\omega_{st}}{e^{-sz_i}+1} + \frac{\omega_{sw}}{e^{sz_i}+1} \tag{2}$$

where ω switches between two different values, the stance frequency, ω_{st}, and the swing frequency, ω_{sw}, based on the sign of z_i. The switching velocity is determined by the value of s. In general, it is possible to obtain a desired gait by independently modulating both frequencies.

In this work, we achieve inter-limb rhythmical synchronization by non-diffusive coupling the nonlinear oscillators. Coupling has a positive impact on the stability of the oscillator frequency, and eases synchronisation in the presence of noise [28]. The coupling amongst neighbouring oscillators is as follows:

$$\begin{bmatrix} \dot{x}_i \\ \dot{z}_i \end{bmatrix} = \begin{bmatrix} \alpha(\mu_i - r_i^2) & -\omega \\ \omega & \beta(\mu_i - r_i^2) \end{bmatrix} \begin{bmatrix} x_i \\ z_i \end{bmatrix} + \begin{bmatrix} 0 \\ \sum k_{ij}(z_i + \lambda_{ij} z_j) \end{bmatrix} \tag{3}$$

where $i, j \in \{\mathrm{L}_1, \mathrm{L}_2, \mathrm{L}_3, \mathrm{R}_1, \mathrm{R}_2, \mathrm{R}_3\}$, $k_{ij} \in [0, 1]$ is the diffusive coupling term and λ_{ij} is the coupling coefficient that defines the effect of the ith oscillator on the jth oscillator, which establishes phase relationships between them [25]. The value of λ_{ij} is set to 1 if the oscillators excite each other and to -1 if the oscillators inhibit each other [5]. We chose a coupling such that the tripod gait is stable. Figure 4 illustrates the generated $\dot{x}_i$ and $\dot{z}_i$ trajectories of such oscillator-based network.

Following the CASN distribution previously introduced, we propose a decentralised CPG network composed of six CPG-units. Each is immediately connected with its corresponding upper-level ASN, whose outputs represent the amplitude of the oscillator μ, the swinging frequency, ω_{sw}, and the stance frequency, ω_{st}. The CPG network mimics the coupling between ASNs and the crosstalk probability, C_p, becomes the diffusive coupling term k_{ij}. Using this approach the behaviours arising in the CASN are directly translated into gait trajectories (see Fig. 5).

D. Inverse Kinematics

Since our interest focuses on the mechanisms that underpin the generation of adaptable gait patterns, we aim to reliably convert rhythmic gait trajectories into limb movements. This section describes the bottom layer of the proposed architecture, which employs inverse kinematics to calculate the joint angles of a 4-DOF limb (see Fig. 6) from sampled points of a gait

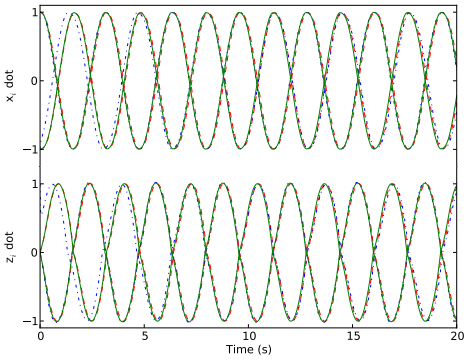

Fig. 4: Generated $\dot{x}_i$ (upper graph) and $\dot{z}_i$ (bottom graph) trajectories of an oscillator-based network. The network is composed of six non-diffusive coupled oscillators. Trajectories obtained for aleatory k_{ij} and constant $\omega_{st} = 2\,\mathrm{rad} \cdot \mathrm{s}^{-1}$, $\omega_{sw} = 2\,\mathrm{rad} \cdot \mathrm{s}^{-1}$, $\mu = 1$, $\alpha = 5$ and $\beta = 50$. Notice that non-diffusive coupling favours entrainment between oscillators.

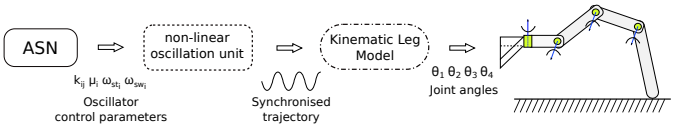

Fig. 5: Each unit-ASN takes sensory information and outputs a set of parameters that modulate the generated trajectory of each nonlinear oscillator unit. Likewise, the kinematic layer samples each trajectory to obtain every joint angle and thereby controls the hexapodal locomotion.

trajectory. These points describe the position and orientation of a limb's tip in Cartesian space. The sampling rate s_r determines the number of points used to map a gait trajectory during a cycle.

The transformation of gait trajectories into joint angles must consider a number of factors:

- The height of the robotic leg remains constant during the stance (descending) phase.
- The y-axis orientation of the robot in rhythmical and synchronized gait trajectories, where the duration of the stance and swing phase have equal duration, is 0.
- The oscillation frequency and amplitude modulate the gait's height and length respectively.

With these assumptions the global orientation of the robot stems from the amplitude and the relationship among the stance and swing phases of every robot leg. In order to achieve independence between the gait's height and length, we control the trajectory of the ith coxa joint (gait length) using the generated $\dot{x}_i$ solution and the trajectory of the ith femur, tibia and tars joints (gait height) using the generated $\dot{z}_i$ solution. Sampled points are expressed as $(x_i, 0, z_i)$ to accomplish the inverse kinematics. Figure 7 shows the rhythmic gait trajectory used in the inverse kinematic layer.

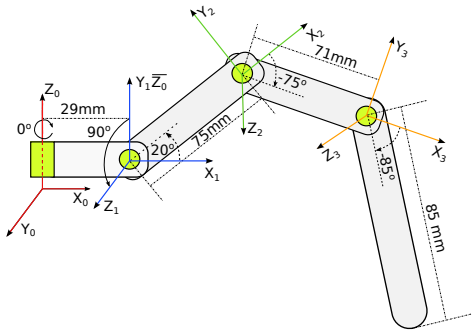

Fig. 6: Illustration of the 4-DOF leg used in our research, showing the arrangement of coordinates frames. Its four rotational joints are distributed as follows: a perpendicular joint followed by three parallel joints. In an attempt to simplify the inverse kinematic problem, we supply the robot with a constant WARTG angle (Wrist Angle Relative to Ground) of 175^o. The angles in the figure represent the initial configuration of every joint.

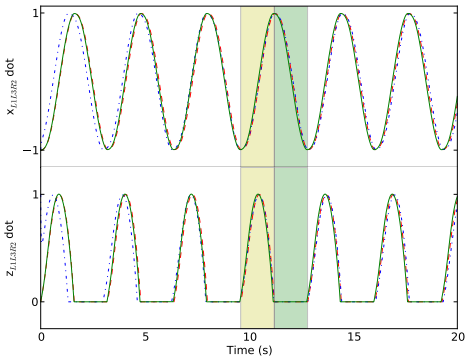

Fig. 7: Modulated $\dot{x}$ and $\dot{z}$ solution of the L1, L3 and R2 nonlinear oscillators. Trajectories obtained for aleatory k_{ij} and constant $\omega_{st} = 2\text{rad}\cdot\text{s}^{-1}$, $\omega_{sw} = 2\text{rad}\cdot\text{s}^{-1}$, $\mu = 1$, $\alpha = 5$ and $\beta = 50$. The green and yellow coloured areas are the swing and stance phases respectively. During the swing phase the robotic limbs move forward (upper graph) while describing an elliptical arc (bottom graph), which starts at $\dot{x} = -1$ and reaches its peak at $\dot{x} = 0$. Likewise, the limb returns to the stance phase when $\dot{x} = 1$. On the contrary, the robotic limbs collide with the ground ($\dot{z} = 0$) while moving backwards along the stance phase.

III. Evolving Coupled Artificial Signalling Networks

CASNs are evolved using a standard generational evolutionary algorithm with tournament selection (size = 4), uniform crossover (rate = 0.3), and point mutation (rate = 0.05). A multi-chromosomal encoding is used to evolve CASNs. This representation counteracts problems with growing complexity and increases modularity. In particular, this enables complex problems to be divided into smaller tasks, which improves the evolution of complex structures [29] and permits the inclusion of independent and different computational representations [30].

A CASN is encoded as an indexed sequence of chromosomes, each of which defines an ASN. We used an standardised genetic encoding for all ASNs (see Fig. 8). This represents the ASN as an indexed sequence of enzymes followed by timing information. Crossover points lie between enzyme boundaries and chromosome shuffling is not permitted. In a attempt to reduce the complexity of the networks the number of enzymes of each ASN was fixed at 10. Inputs and outputs (S_i and P_i) are represented by their absolute indices. Chemical concentrations and mapping parameters are described using floating-point numbers and mutated using a Gaussian function with its centre at the current value. Continuous values introduce two main advantages. First, they ease the coupling with the external environment, thus inputs and outputs do not require an alternative encoding. Second, they discourage fast convergence to static orbits by permitting an infinite state space (within the limits of representation). This underpins the emergence of more complex network dynamics and increases expressiveness. Finally, mutation is restricted to the operations described in [31], to embrace biochemical plausibility in the evolution of interaction graphs.

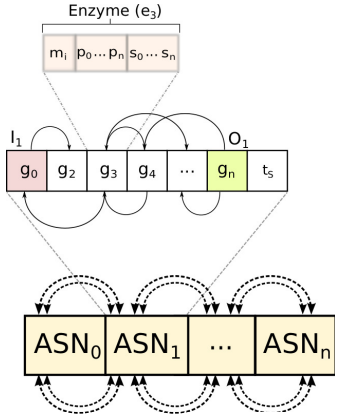

Fig. 8: Genetic Encoding of a coupled artificial signalling network.

IV. Controlling Legged Robot Locomotion

A simulated model (see Fig. 9) of the real robot T-Hex is used to evaluate our architecture [32]. The T-Hex is a 24 DOF hexapod robot developed by Lynxmotion. This robot has four joints per leg connected by actuators at the corner. In this work we follow the limb conventions introduced in [33]. Limbs on the left (L) and right (R) sides of the hexapod are numbered from front to rear starting at 1. The robot is initially configured using the tripod gait, which has a duty factor of 0.5. On each segment, contralateral limbs are 180^o out of phase. Adjacent limbs on each side are also 180^o out of phase. Hence, three legs moves simultaneously in each step. The limited adaptability of the tripod gait is used to assess the capacity of our system to adaptively modulate locomotion patterns using environmental feedback.

The robot was simulated using the Open Dynamics Engine (ODE) physics engine, with a step size of $\Delta_t = 0.01$, friction of $100N$, CFM (an ODE parameter) of 10^{-5}, and standard gravity. Actuators have maximum angular velocity of $4ms^{-1}$ and a maximum torque of $45Nm$. Their movements are limited in both the z-axis plane for the coxa joint and the x-axis plane for the femur, tibia and tar joints, to a maximum rotation of 90^o and a minimum of -90^o. The robot is complemented with six contact sensors, on the tip of every leg, and six ultrasound sensors, which are located above each leg in an elliptical base on top of the robot body. These values are sufficient to mimic the characteristics of the real robot. In addition, a rough terrain is simulated by a set of box-like shapes. Each shape is randomly created with a maximum height of 0.11 ODE units and rotation of 45^o.

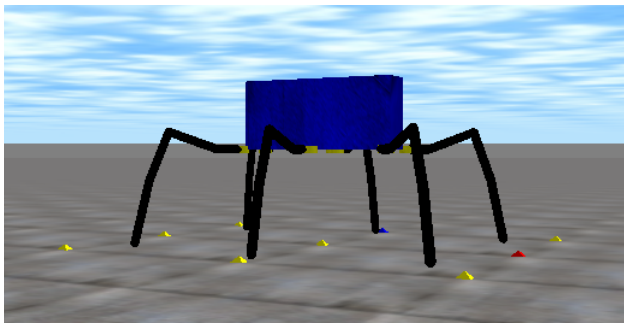

Fig. 9: Simulated T-Hex robot in Open Dynamics Engine.

The coupled oscillators are randomly initialized and numerically integrated using the fifth-order Dormand-Prince method with a step size of $\Delta_t = 0.01$. The generated gait trajectory is scaled to a maximum height of 70mm, a maximum length of 60mm, with a sampling rate of $s_r = \pi/2$ (≈ 80 integration time steps). These values prevent legs collisions. The CASN is executed every 22 simulation steps (time the simulated robot needs to perform each movement).

We use a rough terrain to test the performance of our model. The task was to evolve CASNs capable of controlling the robot when walking over rough terrains. The main purpose of this task is to determine the ability of the CASN to express different behaviours to generate adaptive gaits trajectories. The population size is 500, with a generation limit of 200. The fitness of the robot controllers is the Euclidean distance moved in a straight line during a period of 2000 time steps.

Each ASN in the CASN has four inputs, corresponding to the leg contact sensor and the three lateral ultrasound sensors, and two outputs, which are used to modulate the frequency and amplitude of a CPG unit between each CASN update. To compensate for the lack of lateral walks, ultrasound sensors feed the ASNs with noise readings in the interval $[0.9, 1.0]$. All outputs are linearly scaled in the ranges $[0, 2]$ for the amplitude and $[1, 8]$ for the frequency. The inputs of the ASNs are delivery through substrate concentrations.

V. Results

When the signalling network layer is not used (i.e. the oscillator parameters are kept constant), the furthest distance achieved by the robot in the evaluation period was 3.47 ODE units on the uneven terrain using maximum amplitude and a frequency of $\omega = 4\,\text{rad} \cdot \text{s}^{-1}$. Figure 10 shows, by comparison, the fitness distributions over 30 runs for robots controlled by evolved CASNs. From this plot, it is clear that evolved controllers can move significantly further over uneven terrain than a non-adaptive controller. Figure 10 also shows the best distances achieved by random solutions from the first generation in each of the 30 runs, suggesting that this performance improvement does not come about through the use of modulation alone, but rather through specific evolved patterns of modulation. An example of a robot being controlled by an evolved CASN in shown in Figure 11.

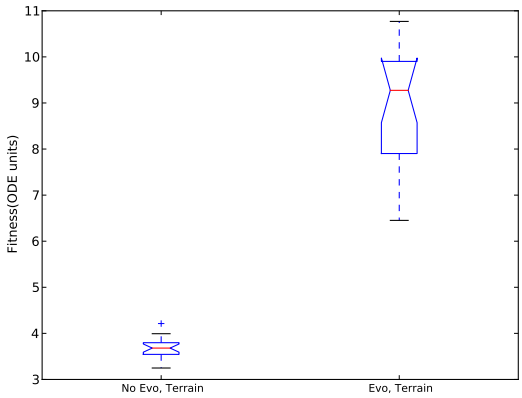

Fig. 10: Controlling legged robot using evolve and non-evolved CASN when facing rough terrains. Summary of statistics for 30 runs are shown as box plots.

Notably, CASNs appear able to dynamically express different behaviours when faced with changing environments, such as when moving from the flat part of the terrain to the uneven section. This is important as it confers the robot the ability to adjust its dynamics in the presence of strong perturbations (i.e. rough terrain), increasing its adaptability. This behaviour reflects the capacity of cellular signalling pathways to produce coordinated and adaptive responses when interacting with one another.

An example of the gait trajectories of an evolved CASN controller on rough terrain is shown in Figure 12. The oscillator trajectories maintain periodicity and synchronisation despite being independently modulated. Although it is a consequence of the tripod coupling of the CPG-units, this also emphasises the role of parameter modulation in order to obtain effective gaits. In general, the ratio between the stance phase and the swing phase leads to different type of gaits. This is a consequence of subtle changes in the swing phase duration while keeping the stance phrase practically constant. We can observe a similar behaviour in Figure 13.

Figure 11 illustrates how adaptive modulation of the locomotion parameters affects the robot when travelling to and

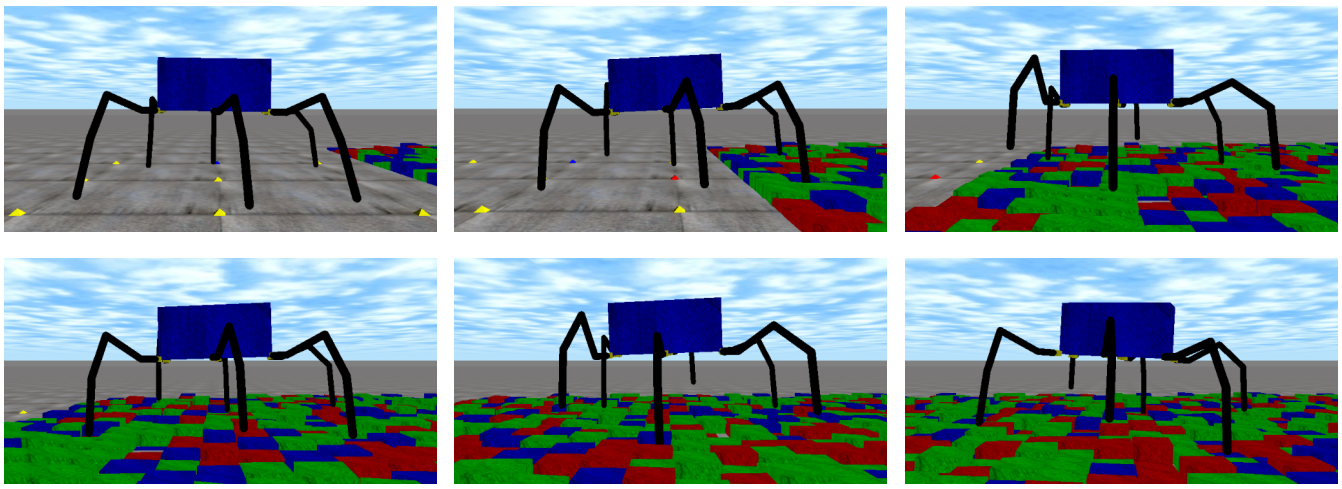

Fig. 11: Sequence of walking of the simulated robot on an uneven terrain. There is an interval of 400ms between each snapshot.

then over an uneven terrain. Initially, the robot must stabilise its internal dynamics in order to achieve forward locomotion. After 344 ms, the left front leg of the robot contacts the terrain, (leg L1), which changes the robot's internal behaviour. This mainly occurs in legs $L3$ and $R2$ (see Fig. 12). The robot manages to fully stand on the terrain at simulation time of $t \approx 1000$ms (equivalent to $t_s \approx 30$). Once the robot starts walking over the terrain, changes in the amplitude and swing frequency denote alteration in the robot's internal dynamics (see Fig. 13 after the $\approx 35 - th$ modulation).

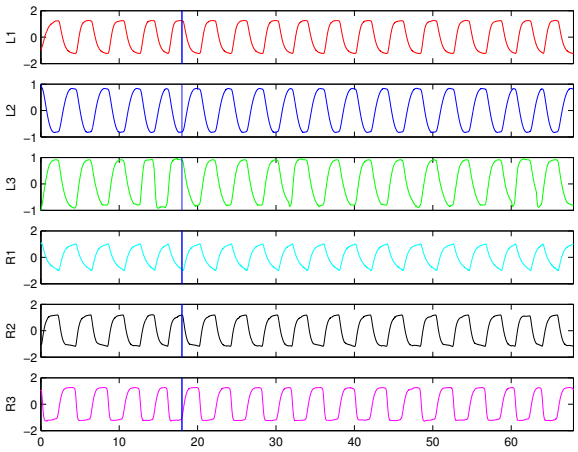

Fig. 12: Examples of CPGs trajectories modulated by an evolved CASN. The top three and bottom three patterns correspond to the left and right legs respectively. The blue vertical line indicates the time step where the robot (leg $L1$) contacts the uneven terrain ($t_s = 17.2$). At this time, the leg $L1$ finishes its swing (ascending) phase and commences the stance (descending) phase.

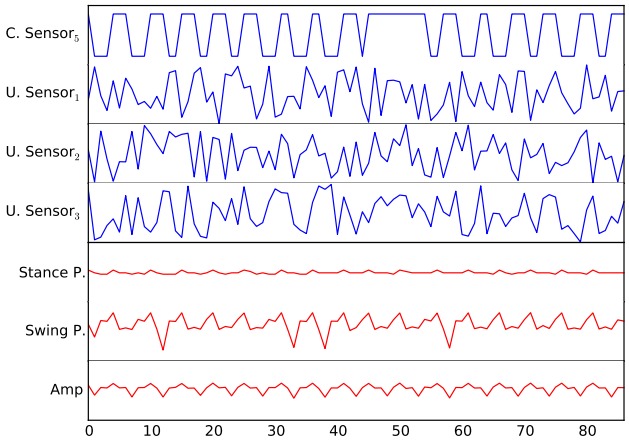

Fig. 13: ASN_5 inputs (four upper graphs) and outputs (three bottom graphs) after begin updated. The inputs are used to modulate the locomotive trajectory $L5$ in Figure 12. Note that the networks are updated every 22 ms.

VI. Conclusion

In this paper, we have shown that coupled artificial signalling networks can be evolved to generate the locomotion patterns of a six-legged robot. Our approach is inspired by cellular signalling pathways, the biochemical mechanisms which transduce changes in a cell's environment into changes in a cell's activities. In particular, we used a three-layer architecture to translate control directives into joint movements. An upper layer comprised a coupled artificial signalling network, which translates sensory information into internal parameter changes. These parameters then modulate the behaviour of the middle layer, which generates rhythmic gait trajectories by combining the x and z solutions of a network of coupled Hopf oscillators. The final layer calculates the desired joint

angles by solving the inverse kinematic problem for the robot. We have illustrated the utility of this architecture by showing how it improves the locomotion of a simulated robot over an uneven terrain, using an evolutionary algorithm to design coupled artificial signalling networks with suitable behaviours. Analysis of the resulting controllers suggests that these networks show sensitivity and robustness to sensory stimuli in slow-changing complex environments.

This work also shows how coupled artificial signalling networks can decompose problems in which variables have a strong dependence, reducing them to smaller, weakly-coupled, tasks. Motion in legged robots is one of these problems, since limbs need to coordinate with each other in an specific manner in order to achieve locomotion. We explored this property through a decentralised controller where each artificial signaling network and CPG unit was responsible for each leg's motion.

Additionally, we found that coupled signalling networks are able to dynamically adjust the gait pattern of each leg based on sensory feedback. Without limiting the modulation of the stance and swing phase, the network was able to maintain constant the swing phase while adjusting the stance phase. In future work, we plan to use a real robot to test our architecture, and apply this approach to robotic control within complex real-world environments.

ACKNOWLEDGMENT

This research is supported by the EPSRC-funded project (ref: EP/F060041/1) Artificial Biochemical Networks: Computational Models and Architectures.

REFERENCES

[1] M. A. Schwartz and V. Baron, "Interaction between mitogenic stimuli, or, a thousand and one connections," *Current Opinion in Cell Biology*, vol. 11, no. 2, pp. 197–202, 1999.

[2] M. Frasca, P. Arean, and L. Fortuna, "Bio-Inspired Emergent Control of Locomotion Systems," in *World Scientific series on Nonlinear Science*, ser. A. Word Scientific, December 2004, vol. 48, p. 197.

[3] G. Capi, Y. Nasu, L. Barolli, K. Mitobe, and K. Takeda, "Application of genetic algorithms for biped robot gait synthesis optimization during walking and going up-stairs," *Advanced Robotics*, vol. 15, no. 6, pp. 675–694, 2001.

[4] R. C. Moioli, P. A. Vargas, and P. Husbands, "A multiple hormone approach to the homeostatic control of conflicting behaviours in an autonomous mobile robot," in *Proceedings of the Eleventh conference on Congress on Evolutionary Computation*, ser. CEC'09. Piscataway, NJ, USA: IEEE Press, 2009, pp. 47–54.

[5] C. Liu, Q. Chen, and J. Zhang, "Coupled van der pol oscillators utilised as central pattern generators for quadruped locomotion," in *Control and Decision Conference, 2009. CCDC '09. Chinese*, June, pp. 3677–3682.

[6] L. Righetti and A. J. Ijspeert, "Design methodologies for central pattern generators: an application to crawling humanoids," in *Proceedings of Robotics: Science and Systems*, 2006, pp. 191–198.

[7] S. Aoi and K. Tsuchiya, "Stability analysis of a simple walking model driven by a rhythmic signal," in *Proc. of the IEEE/RSJ Int. Conf. on Intelligent Robots and Systems (IROS2004*, 2004.

[8] A. C. de Pina Filho, M. S. Dutra, and L. S. C. Raptopoulos, "Modeling of a bipedal robot using mutually coupled rayleigh oscillators," *Biological Cybernetics*, vol. 92, no. 1, pp. 1–7, 2005.

[9] M. Habib, G. L. Liu, K. Watanabe, and K. Izumi, "Bipedal locomotion control via cpgs with coupled nonlinear oscillators," in *Mechatronics, ICM2007 4th IEEE International Conference on*, May, pp. 1–6.

[10] R. Moioli, P. A. Vargas, and P. Husbands, "Exploring the Kuramoto Model of Coupled Oscillators in Minimally Cognitive Evolutionary Robotics Tasks," in *WCCI 2010 IEEE World Congress on Computational Intelligence - CEC IEEE*, 2010, pp. 2483–2490.

[11] L. I. company, "4dof t-hex combo kit for bot board/ssc-32/bap28," Available at http://www.lynxmotion.com/c-151-t-hex-4-dof.aspx.

[12] M. J. Fisher, R. C. Paton, and K. Matsuno, "Intracellular signalling proteins as 'smart' agents in parallel distributed processes," *BioSystems*, vol. 50, pp. 159–171, 1999.

[13] D. Bray and S. Lay, "Computer simulated evolution of a network of cell signalling molecules," *Biophysical*, vol. 66, pp. 972–977, 1994.

[14] P. Husbands, A. Philippides, P. Vargas, C. L. Buckley, P. Fine, E. Di Paolo, and M. O'Shea, "Spatial, temporal, and modulatory factors affecting gasnet evolvability in a visually guided robotics task," *Complex.*, vol. 16, no. 2, pp. 35–44, Nov. 2010.

[15] A. Deckard and M. H. Sauro, "Preliminary studies on the *in silico* evolution of biochemical networks," *Biochemistry*, vol. 5, no. 10, pp. 1423–1431, 2004.

[16] L. A. Fuente, M. A. Lones, A. P. Turner, L. S. Caves, S. Stepney, and A. M. Tyrrell, "Evolved artificial signalling networks for the control of a conservative complex dynamical system," in *9th International Conference on Information Processing in Cells and Tissues (IPCAT 2012) Cambridge, UK*, ser. LNCS, vol. 7223. Springer, 2012, pp. 38–49.

[17] L. A. Fuente, M. A. Lones, A. P. Turner, S. Stepney, L. S. Caves, and A. M. Tyrrell, "Computational models of signalling networks for non-linear control," *Biosystems*, no. 0, 2013.

[18] M. A. Lones, L. S. Caves, S. Stepney, and A. M. Tyrrell, "Controlling complex dynamics with artificial biochemical networks," in *EuroGP 2010, Istanbul, Turkey, April 2010*, ser. LNCS, vol. 6021. Springer, 2010.

[19] M. A. Lones, A. M. Tyrrell, S. Stepney, and L. S. D. Caves, "Controlling legged robots with coupled artificial biochemical networks," in *ECAL 2011, Paris, France, August 2011*. MIT Press, 2011, pp. 465–472.

[20] M. A. Lones, L. A. Fuente, A. P. Turner, L. S. D. Caves, S. Stepney, S. L. Smith, and A. M. Tyrrell, "Artificial biochemical networks: Evolving dynamical systems to control dynamical systems," *IEEE Transactions on Evolutionary Computation*, 2013.

[21] L. Bull, "A simple computational cell: coupling Boolean gene and protein networks," *Artificial Life*, vol. 18, no. 2, pp. 223 – 236, 2012.

[22] M. Hucka, A. Finney, Sauro *et al.*, "The systems biology markup language (sbml): a medium for representation and exchange of biochemical network models," *Bioinformatics*, vol. 19, no. 4, pp. 524–531, 2003.

[23] L. Righetti and A. J. Ijspeert, "Pattern generators with sensory feedback for the control of quadruped locomotion," in *Proceedings of the 2008 IEEE International Conference on Robotics and Automation (ICRA 2008)*, 2008, pp. 819–824.

[24] C. P. Santos and V. Matos, "Gait transition and modulation in a quadruped robot: A brainstem-like modulation approach," *Robotics and Autonomous Systems*, vol. 59, no. 9, pp. 620 – 634, 2011.

[25] J. Wright and I. Jordanov, "Intelligent approaches in locomotion," in *Neural Networks (IJCNN), The 2012 International Joint Conference on*, June, pp. 1–8.

[26] G. S. Hornby, S. Takamura, T. Yamamoto, and M. Fujita, "Autonomous evolution of dynamic gaits with two quadruped robots," *IEEE Transactions on Robotics*, vol. 21, pp. 402–410, 2005.

[27] R. Campos, V. Matos, and C. Santos, "Hexapod locomotion: A nonlinear dynamical systems approach," in *IECON 2010 - 36th Annual Conference on IEEE Industrial Electronics Society*, Nov., pp. 1546–1551.

[28] J. Hale, "Diffusive coupling, dissipation, and synchronization," *Journal of Dynamics and Differential Equations*, vol. 9, pp. 1–52, 1997.

[29] R. Cavill, S. Smith, and A. M. Tyrrell, "Multi-chromosomal genetic programming," in *In Proc. of the 2005 Genetic and Evolutionary Computation Conference*. ACM Press, 2005, pp. 1649–1656.

[30] H. A. Mayer and M. Spitzlinger, "Multi-chromosomal representations and chromosome shuffling in evolutionary algorithms," in *Evolutionary Computation, 2003. CEC '03. The 2003 Congress on*, vol. 2, dec. 2003, pp. 1145–1149.

[31] J. Ziegler and W. Banzhaf, "Evolving control metabolisms for a robot," *Artificial Life*, vol. 7, pp. 171–190, 2001.

[32] L. I. company, "Lynxmotion robotic toolkit," Available at http://www.lynxmotion.com/.

[33] J. Collins and I. Stewart, "Hexapodal gaits and coupled nonlinear oscillator models," *Biological Cybernetics*, vol. 68, pp. 287–298, 1993.